Silver Chloride Crystals," *J. Electrochem. Soc.*, **109**, 745 (1962).
Grim, E. and K. Sollner, "True Anomalous Osmosis in Multi-Solute Model Membrane Systems," *J. Gen. Physiol.*, **44**, 381 (1960).
Hansen, R., and M. Anderson, "Anomalous Osmosis in Dialysis of Acids with Anion Exchange Membranes," *Ind. Eng. Chem. Fundamentals*, **6**, 543 (1967).
Kedem, O., and A. Katchalski, "A Physical Interpretation of the Phenomenological Coefficients of Membrane Permeability," *J. Gen. Physiol.*, **45**, 143 (1961).
Lakshminarayanaiah, N., *Transport Phenomena in Membranes*, Academic Press, New York and London (1969).
Lippman, G., "Endosmose entre deux Liquides de Meme Composition Chimique et de Temperatures Differentes," *Compt. Rend.*, **145**, 104 (1907).
Mackay, D., and P. Meares, "The Electrical Conductivity and Electroosmotic Permeability of a Cation-Exchange Resin," *Trans. Faraday Soc.*, **55**, 1221 (1959).
Millero, F., *The Partial Molal Volume of Electrolytes in Aqueous Solutions*, Rosenstiel School of Marine and Atmospheric Sciences, University of Miami, Florida (1970).
Praissman, M., I. Miller, H. Gregor, and J. Berkowitz, "Ion-Mediated Water Flow, II. Anomalous Osmosis," *J. Memb. Biol.*, **11**, 153 (1973).
Rastogi, R., R. Blokhra, and R. Agarwal. "Cross-Phenomenological Coefficients, Part I. Studies on Thermo-osmosis," *Trans. Faraday Soc.*, **60**, 1386 (1964).
Tasaka, M., Y. Kondo, and M. Nagasawa, "Anomalous Osmosis Through Charged Membranes," *J. Phys Chem.*, **73**, 3181 (1969).
Tombalakian, A., M. Worsley, and W. Graydon, "Solvent Mass Transfer Across Ion-Exchange Membranes," *J. Am. Chem. Soc.*, **88**, 661 (1966).
Toyoshima, Y., Y. Kobatake, and H. Fujita, "Studies of Membrane Phenomena," *Trans. Faraday Soc.*, **63**, 2828 (1967).
Voellmy, H., and P. Läuger, "Untersuchungen uber Thermoosmose in Flussigkeiten," *Ber. Bunsengesell.*, **70**, 165 (1966).
Weinstein, J., and S. Caplan, "Charge-Mosaic Membranes: Enhanced Permeability and Negative Osmosis With a Symmetrical Salt," *Science*, **5**, 70 (1968).

Manuscript received May 17, 1974; revision received and accepted November 18, 1974.

Onset of Fluidization and Slugging in Beds of Uniform Particles

A comprehensive investigation has been made of the boundaries of the regime of bubbling aggregative fluidization. Experiments were done with sand, glass beads, clover seed, and iron shot fluidized with helium, air, and freon-12 in columns 2.5, 5, 10, and 21 cm in diameter. Bed heights ranged from 1 to 60 column diameters, particle diameters from 0.07 to 1.1 mm, particle densities from 1300 to 7600 kg/m^3, and gas densities from 0.17 to 5.2 kg/m^3. Correlations are presented for the void fraction at the minimum bubbling point and for the superficial fluid velocity at the points of minimum fluidization, minimum bubbling, and minimum slugging.

T. E. BROADHURST
and
H. A. BECKER

Department of Chemical Engineering
Queen's University
Kingston, Ontario, Canada

SCOPE

Fluidization of a bed of particles occurs when the particles are effectively suspended in a stream of fluid flowing through the bed, that is, their weight is balanced by the buoyancy and drag due to the fluid. Under certain conditions, normally in fluidization by gases, the regime called *aggregative fluidization* is observed which is characterized by the appearance of two phases: a dense phase in which the voidage is about the same as in the bed at the onset of fluidization, and a dilute phase in which the particle population is very sparse. At moderate fluid flow rates the dense phase is continuous and the dilute phase characteristically takes the form of a stream of rising bubbles. With increasing flow rate, however, a point may be reached where bubbles appear that extend across the bed; these bubbles are called *slugs*, and the condition is referred to as *slugging*. The practically useful regime of aggregative fluidization is bounded by the beginning of bubbling at low superficial fluid velocities and by the onset of slugging at high velocities. The bed-mixing action of the bubbles is responsible for most of the technical advantages of aggregative fluidization. The occurrence of slugging is accompanied by marked deterioration in both the quality of bed mixing and the quality of gas-particle contacting. The passage of slugs out of the bed, moreover, produces large pressure fluctuations and pounding which can be mechanically damaging to equipment.

It is thus practically important to be able to predict the limits of the regime of good aggregative fluidization. Attention is focused on: (1) the point of minimum bubbling, most precisely defined by aggregatively fluidizing a bed and then gradually reducing the fluid flow rate to the point where bubbles no longer appear, and (2) the point of minimum slugging, defined as the point at which

Correspondence concerning this paper should be addressed to H. A. Becker. T. E. Broadhurst is with Imperial Oil Enterprizes Ltd., Sarnia, Ontario, Canada.

bubbles emerging from the bed span the breadth of the bed (nonvisual definitions are also possible, based, for example, on measurements with pressure transducers). Past studies of the onset of fluidization have emphasized the point of minimum fluidization, defined in terms of the change in pressure drop characteristics observed in passing from the fluidized state to the fixed-bed state. A systematic study of the onset of slugging has not previously been reported. In the present work, experiments were carried out with wide ranges of column diameter, bed depth, particle diameter and density, and gas properties. The points of minimum fluidization, minimum bubbling, and minimum slugging were observed, and generalized correlations of the results were sought by means of statistical analysis in combination with the theory of dimensionless groups.

CONCLUSIONS AND SIGNIFICANCE

The results show that the superficial fluid velocity at the point of minimum slugging v_{ms} depends strongly on the ratio of bed height and column diameter. This dependency does not appear in the hitherto accepted criteria for the occurrence of slugging, and it is evident that these generalizations were based on insufficient data. The ratio of the gas and particle densities also exerts an effect, small but significant, and previously unrecognized. The minimum slugging velocity increases with increasing particle diameter, but not as rapidly as the minimum bubbling velocity v_{mb}. Thus the difference $v_{ms} - v_{mb}$ is relatively small for large particles, and the regime of good aggregative fluidization is correspondingly smaller in extent. The minimum slugging velocity decreases with increasing bed height, but the rate of decrease is (1) smaller for large particles than for small ones, and (2) smaller for dense particles than for light ones.

The minimum fluidization velocity v_{mf} tends to be slightly larger than the minimum bubbling velocity v_{mb}, but the differences are practically unimportant.

The experiments effectively covered the whole range of practical conditions, with the exceptions that (1) the largest column diameter was 21 cm, whereas some industrial units are over 5 m in diameter, and (2) the highest bed loading was about 10,000 kg/m^2 (a 2 m high bed of iron shot). The theory of dimensionless groups was rigorously applied in analyzing the results, and there is no indication in the structure of the correlations obtained that they may not be valid for any reasonable conditions; that is, it appears unlikely that study of beds of very large diameter or very high loading will substantially alter the conclusions.

The generalized correlations for v_{ms}, v_{mb}, and v_{mf} are the principal results of the work, and have been expressed in equation form. A reliable correlation for v_{ms} was not previously available. The correlation for v_{mf} shows good agreement with the results of Leva. A correlation for v_{mb} was previously lacking; it was generally assumed that v_{mb} and v_{mf} are practically equal, and the present work shows that this assumption is reasonably good, if not entirely correct.

BASIC CONSIDERATIONS FOR DESIGNING EXPERIMENTS AND FORMULATING CORRELATIONS

The existing mechanistic models, such as Stewart and Davidson's model for the onset of slugging (1967), help with understanding the phenomena but do not provide a sufficient basis for planning experiments and correlating experimental data. It was concluded in the present work that the most practical approach is still by a rigorous similitude analysis in which, among the various equivalent sets of dimensionless groups that are possible, an optimum set is chosen. The choice is based on both theoretical and empirical considerations.

The various characteristic variables, or forces and lengths, were examined, and the following set of dimensionless groups was formed by taking ratios of forces and of lengths:

$$\{\rho_f v D_p/\mu,\ \rho_f v^2/\gamma D_p,\ \rho_p/\rho_f,\ \rho_p g H_0/P_1,\ D_p/H_0,\ D_p/D,\ \epsilon,\ \psi\}$$

The fluid velocities v and bed void fractions ϵ of interest, namely those at the points of minimum fluidization, minimum bubbling, and minimum slugging, are dependent variables. Hence the void fraction ϵ, the Reynolds number $Re \equiv \rho_f v D_p/\mu$, and the modified Froude number $Fr \equiv \rho_f v^2/\gamma D_p$ are all dependent-variable groups. However, Re and Fr can be combined in such a way that v cancels, yielding an independent-variable group that must be considered: the Archimedes number, $Ar \equiv \rho_f \gamma D_p^3/\mu^2$; $Ar \equiv Re^2/Fr$. The set **X** of independent-variable groups is thus found to be

$$\mathbf{X} = \{\rho_f\gamma D_p^3/\mu^2,\ \rho_p/\rho_f,\ \rho_p g H_0/P_1,\ D_p/H_0,\ D_p/D,\ \psi\} \tag{1}$$

We next consider the set of dependent-variable groups, **Y**. The above introduction of the Archimedes number has the general consequence that a set of two dependent-variable groups $\{Re, Fr\}$ is replaced by an equivalent set consisting of Ar and either Re or Fr. The choice between Re and Fr is mathematically arbitrary, but physically Fr is preferable; particle weight minus buoyancy, represented by Fr, is important in all regimes of the phenomena considered, whereas the viscous forces, represented by Re, are not. The set of dependent-variable groups is thus taken to be

$$\mathbf{Y} = \{\rho_f v^2/\gamma D_p,\ \epsilon\} \tag{2}$$

It follows from the theory of dimensionless groups that the correlations to be sought between the dependent and independent variables must be of the general form

$$Y_i = Y_i(\mathbf{X}) \tag{3}$$

where $Y_1 \equiv \rho_f v^2/\gamma D_p$ and $Y_2 \equiv \epsilon$.

The reciprocal of the modified Froude number $\gamma D_p/\rho_f v^2$ behaves rather like a particle drag coefficient in the present context. The Archimedes number $\rho_f\gamma D_p^3/\mu^2$ can be interpreted as the square of the characteristic Reynolds number of the system, the characteristic (independent-variable) velocity being $\sqrt{(D_p\gamma/\rho_f)}$. The group ρ_p/ρ_f relates to accelerated motion and expresses the ratio of particle inertia to fluid inertia. The groups D_p/D, D_p/H_0, and ψ are obvious characteristics of the system geometry. The group $\rho_p g H_0/P_1$ characterizes, in the case when the fluid is an ideal gas, the change in gas density across the bed due to the change in pressure. If nonideal gas behavior is important, then the pressure ratio P_1/P_c and the temperature ratio T_1/T_c should be added to (1), where the subscript c refers to the thermodynamic critical conditions.

The gas density ρ_f was evaluated at the pressure P_1 existing above the bed, and the superficial velocity v was calculated from the mass flow rate and this density.

The quantity H_0 is used as the measure of bed height because any actual height H is always a function of the fraction void ϵ; we have $H_0 \equiv m''/\rho_p = H(1-\epsilon)$, where m'' is the total mass of particles in the bed per unit base area. Both H and ϵ must, strictly speaking, be regarded as dependent variables. However, the constants in the various correlations herein developed are insignificantly affected if the settled bed depth H_s is used in place of H_0; for the systems studied, the transformation

$$H_0 = H_s(1-\epsilon_s), \quad \epsilon_s = 0.40$$

carries a correlation involving H_0 into one involving H_s. The settled bed height is the height of the fixed bed obtained when a bed is consolidated by jarring or vibration until no further settling is observed. Because the bed geometry is more easily visualized in terms of H_s and since the results are not significantly affected thereby, H_s/D is used as the dimensionless group involving bed height in most of the subsequent discussion. In practice, H_0/D may usually be easier to use since it follows directly from knowledge of the bed weight and the particle density; final correlations that involve the bed height as an independent variable are therefore also given in terms of H_0/D.

Other particle shape characteristics besides the sphericity ψ may be important; ψ is however the simplest and, based on experience with sedimentation and flow through porous media, may be adequate.

The theory of dimensionless groups has not always been applied in a rigorous and consistent manner in past investigations. Wilhelm and Kwauk (1945), for example, suggested that the division of regimes between particulate and aggregative fluidization might depend on a Froude number Fr_{mf} based on the minimum fluidization velocity v_{mf}, a dependent variable. Romero and Johansen (1962) proposed, for the same purpose, the Froude number Fr_{mf}, the Reynolds number Re_{mf}, $(\rho_p - \rho_f)/\rho_f$, and H_{mf}/D, thus involving three dependent-variable groups. The ratio v/v_{mf} is also frequently utilized in certain types of correlations. The use of groups involving dependent variables may be mechanistically revealing in some cases, but it is not the best basis for developing generalized correlations. In addition to hypothesizing dependencies on dependent-variable groups, most past analyses have been partial or incomplete, omitting consideration of one or more characteristic independent variables.

The set of independent-variable groups, (1), is large. This condition is indicative of the well-known scale-up difficulties with fluid-bed behavior. For complete dynamic similarity to exist, all dimensionless groups in model and prototype must be constants. For most purposes, this is possible only if model and prototype are identical. Hence, unless it can be shown that some of the groups are weak or unimportant in effect, only partial or distorted modeling is possible. The approach taken in the present work was to use, in the experiments, a wide range of particle densities and sizes, a wide range of fluid properties, and a wide range of column diameters so that nearly the whole range of practical interest was covered. Correlations were then developed with the help of statistical techniques, and no independent variable or group was neglected unless its influence could be shown to be statistically unimportant. Thus the correlations should be quite generally valid, and with known levels of accuracy.

TABLE 1. DENSITY AND VISCOSITY OF GASES AT 20°C AND 1 ATM.

Gas	Density, kg/m^3	Viscosity, 10^5 kg/m s
Helium	0.166	1.98
Air	1.21	1.81
Freon-12	5.2	1.25

TABLE 2. PHYSICAL PROPERTIES OF PARTICLES

Material and supplier	D_p*, mm	ρ_p, kg/m^3	ψ†
Sand; American Graded Sand Co., Paterson, New Jersey	0.343	2650	0.85
	0.213	2660	0.85
	0.184	2660	0.85
	0.150	2660	0.85
	0.106	2670	0.85
	0.071	2680	0.85
Glass beads; Minnesota Mining and Mfg. Company, St. Paul, Minnesota	0.481	2480	1.00
	0.297	2450	1.00
	0.165	2450	1.00
	0.100	2430	1.00
Iron shot; Globe Steel Abrasive Co., Mansfield, Ohio	0.356	7550	0.95
	0.243	7370	0.95
Cracking catalyst; Imperial Oil Ltd., Sarnia, Ontario	0.060	1280	0.95
Clover seed	1.09	1300	0.95

* The coefficient of variation for the diameter of an individual sand particle is ± 20%, and for a glass particle ± 10%.

† The coefficient of variation of ψ for an individual sand particle is ± 10%. The variation of ψ for the other particles is less.

APPARATUS AND MATERIALS

The columns were of perspex tubing, 2.5, 5.0, 10.0, and 21.0 cm inside diameter, with 3 to 4 m of height to accommodate deep beds. The gas distributors, which also provided the base support for each bed, were disks of Feltmetal (Huyck Metal Company) over perforated aluminum plates.

The gases, helium, air, and freon-12 provided the densities and viscosities shown in Table 1. The properties of the solid particles are summarized in Table 2. The only particle property that was not varied over a broad range was the shape; the particles were either spherical, or fairly isometric and nearly spherical. The particle sphericity $\psi \equiv (6V_p/\pi)^{2/3}/(S_p/\pi)$ was estimated from photographs of the particles, by comparison with shapes of known sphericity. Particle density was determined from the weight of a sample and the displacement volume in methanol. For particles larger in diameter than 0.18 mm, the mean particle diameter D_p was calculated as the diameter of an equi-volumed sphere from the mean particle weight in a sample of 100 to 200 particles. For smaller particles, screen analysis was used and D_p was estimated by the method of Kunii and Levenspiel (1969, p. 68).

MINIMUM BUBBLING POINT

Method

A measured weight of particles was loaded into the column. A condition of aggregative fluidization was established, and the gas flow was then slowly reduced until no bubbles were visible at the surface. The bed height and the gas flow rate were observed at this point. The observations were repeated ten times and the sample-mean values of the superficial gas velocity and the void fraction at the minimum bubbling point were calculated from the data. Tables of the original data are on record (Broadhurst, 1972).

Effect of D_p/D

The effect of this group was studied in the four columns with sand beds having $H_s/D = 1/2$, fluidized with air. The results, Figure 1, show that $\rho_f v_{mb}^2/\gamma D_p$ is rather weakly affected by D_p/D. In view of the much stronger effects of some of the other groups to be considered, it was

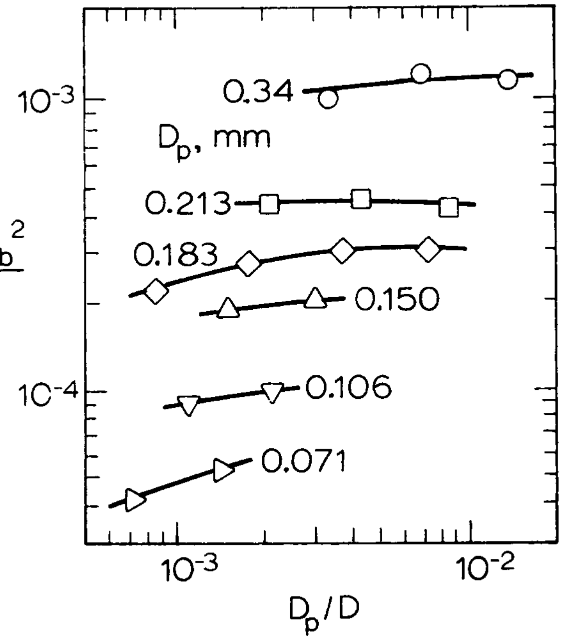

Fig. 1. The effect of D_p/D on the minimum bubbling velocity. The system is sand/air, $\psi = 0.85$, $H_s/D = 1/2$.

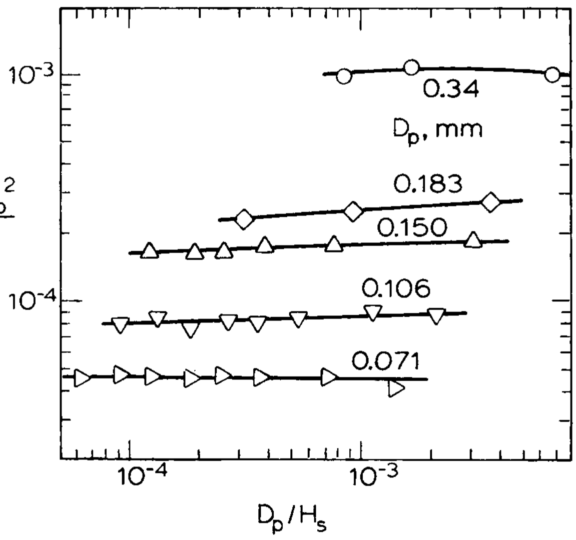

Fig. 2. The effect of D_p/H_s on the minimum bubbling velocity. The system is sand/air, $\psi = 0.85$, $D = 10$ cm.

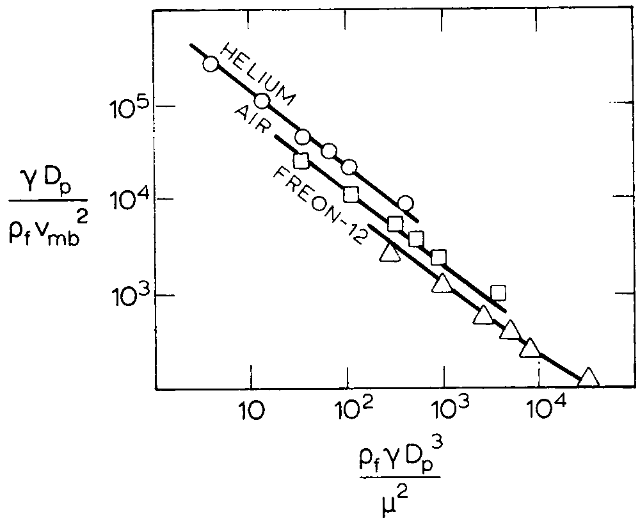

Fig. 3. The relation between the dimensionless minimum bubbling velocity and $\rho_f \gamma D_p^3/\mu^2$. Systems are sand, $\psi = 0.85$, $D = 10$ cm, $H_s/D = 1/2$, fluidization with helium, air, and freon-12.

decided to ignore this dependency altogether.

The effect of D_p/D on the void fraction ϵ_{mb} was found to be insignificant.

Effects of D_p/H_0 and $\rho_p g H_0/P_1$

A series of experiments was carried out in which sand particles of five diameters, at settled bed heights H_s of 5—120 cm, were fluidized in the 10 cm diam. column. The results, Figure 2, indicate that any effects of bed height on $\rho_f v_{mb}^2/\gamma D_p$ are unimportant within normal limits of operation.

Effects of $\rho_f \gamma D_p^3/\mu^2$, ρ_p/ρ_f, and ψ

Variation of the group $\rho_f \gamma D_p^3/\mu^2$ was chiefly effected by varying the particle diameter. The density ratio ρ_p/ρ_f was varied principally through the three gases—helium, air, and freon-12. However, iron shot was studied in addition to the various sands to provide even higher values of ρ_p/ρ_f. The variation of the particle sphericity ψ was small but covered the range encountered in most practical operations. All the tests in this series were done in the 10-cm diam. column with $H_s/D = 1/2$.

A graph of $\gamma D_p/\rho_f v_{mb}^2$ vs. $\rho_f \gamma D_p^3/\mu^2$ for the fluidization of sand particles with helium, air, and freon-12 is shown in Figure 3. The reciprocal of $\rho_f v_{mb}^2/\gamma D_p$ is used as the ordinate because it corresponds to the drag coefficient or friction factor. It is clear that the data for the different gases lie on separate curves, indicating an influence of ρ_p/ρ_f. A graph of all the results is shown in Figure 4. The data for glass spheres lie on the same curves with the sands, indicating negligible effect of the sphericity over the range $0.85 < \psi < 1.00$.

Above the 45° dashed line in Figure 4, representing a Reynolds number of 10, the data are quite collinear for a given value of ρ_p/ρ_f. For the few points where Re_{mb} exceeds 10, there appears to be a tendency for $\gamma D_p/\rho_f v_{mb}^2$ to level off as the flow enters the fully turbulent regime. A model is therefore postulated of the form

$$\frac{\gamma D_p}{\rho_f v_{mb}^2} = A1\left(\frac{\rho_f \gamma D_p^3}{\mu^2}\right)^{A2}\left(\frac{\rho_p}{\rho_f}\right)^{A3} + A4\left(\frac{\rho_p}{\rho_f}\right)^{A5} \quad (4)$$

This model is of the type frequently used for the correlation of friction factors for flow through porous media; for example, the equation of Ergun (1952). The first term on the right represents the creeping flow regime, and the second the fully turbulent. The parameters $A1$ to $A5$ were

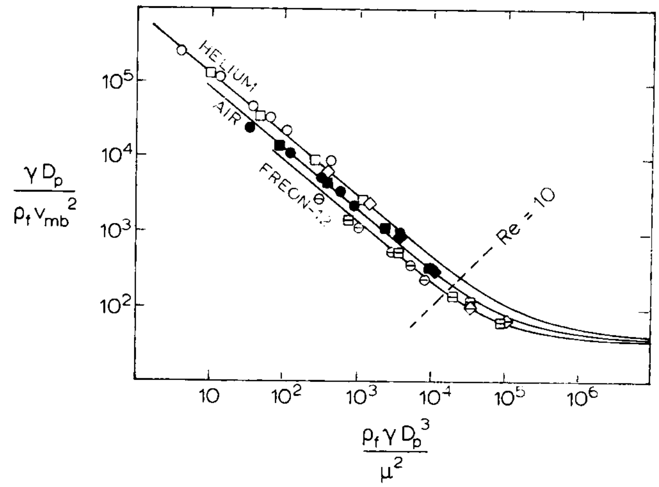

Fig. 4. The relation between the dimensionless minimum bubbling velocity and $\rho_f\gamma D_p^3/\mu^2$. Systems with D = 10 cm, H_s/D = 1/2, fluidization with helium, air, and freon-12. Materials: ○●⊖, sand, ψ = 0.85; □■⊟, glass beads, ψ = 1.00; ◇◆◇, iron shot, ψ = 0.95. Curves are given by Equation (5).

determined by a nonlinear least squares procedure which minimizes the sum of the squares of the residuals. The effect of ρ_p/ρ_f in the second term was found to be insignificant. The resulting equation is

$$\frac{\gamma D_p}{\rho_f v_{mb}^2} = 98000 \left(\frac{\mu^2}{\rho_f \gamma D_p^3}\right)^{0.82} \left(\frac{\rho_p}{\rho_f}\right)^{0.22} + 35.4 \quad (5)$$

$500 < \rho_p/\rho_f < 50000$, and $1 < \rho_f\gamma D_p^3/\mu^2 < 10^7$. The residual variance from this correlation indicates that v_{mb} can be predicted within ± 25% (95% confidence interval) over the range of the data.

For creeping flow, (5) can be written

$$v_{mb} = 0.00319 \left(\frac{\gamma D_p}{\rho_p}\right)^{0.5} \left(\frac{\rho_p \gamma D_p^3}{\mu^2}\right)^{0.41} \left(\frac{\rho_f}{\rho_p}\right)^{0.02} \quad (6)$$

For air/sand systems at 20°C and 1 atm, ρ_p/ρ_f = 2200, and (6) gives

$$v_{mb} = 0.00273 \left(\frac{\gamma D_p}{\rho_p}\right)^{0.5} \left(\frac{\rho_p \gamma D_p^3}{\mu^2}\right)^{0.41} \quad (7)$$

The exponent on ρ_p/ρ_f in (6) is almost insignificantly different from zero, and the differences between the predictions of (6) and (7) over the experimental range of ρ_p/ρ_f, 250—45000, are small. For the systems here studied, $\rho_f/\rho_p << 1$, so that $\gamma/\rho_p \simeq g$. Hence (6) and (7) are, in effect, relations between the Froude number v_{mb}^2/gD_p and the group $\rho_p\gamma D_p^3/\mu^2$. The unimportance of the fluid density ρ_f in these equations for creeping flow is theoretically expected.

The Fraction Void ϵ_{mb}

Because the total variation in the fraction void at the minimum bubbling point is small, the effects of the independent-variable dimensionless groups are effectively revealed by regression analysis. Data on the analysis are summarized in Table 3. The correlation is

$$\epsilon_{mb} = 0.586\, \psi^{-0.72} \left(\frac{\mu^2}{\rho_f \gamma D_p^3}\right)^{0.029} \left(\frac{\rho_f}{\rho_p}\right)^{0.021} \quad (8)$$

$0.85 < \psi < 1$, $1 < \rho_f\gamma D_p^3/\mu^2 < 10^5$, and $500 < \rho_p/\rho_f < 50000$. The particle sphericity, as should be expected, is the major factor determining ϵ_{mb}. The exponents on the last two groups in (8) are small, but each group contributes significantly to reducing the standard error of the estimate.

Measurements of the minimum fluidization velocity v_{mf}, reported in the next section, indicate little difference between it and v_{mb}. It is therefore to be expected that ϵ_{mb} should differ negligibly from ϵ_{mf}, the fraction void at the point of minimum fluidization. Table 4 shows that the predictions of (8) indeed agree very well with Leva's (1959) measurements of ϵ_{mf}, even for sphericities ψ much smaller than those in the present work. The data of Becker (1961), however, indicate inadequacy for very large particles; for these the predicted values are obviously low and quite unrealistic. It thus appears that (8) is valid for systems in the creeping flow regime and somewhat beyond, but not in well-developed turbulent flow. As a general rule, it appears that ϵ_{mb}—or ϵ_{mf}—is predicted by (8) within a probable error of about ± 0.02, provided that the predicted value is larger than 0.37. Values smaller than this are generally less than the settled void fraction for spherical and nearly spherical particles and are physically impossible.

Comparison with Ergun's Equation

The equation of Ergun (1952) for pressure drop across fixed beds is

Table 3. Data on Regression Analysis of the Relation Between the Void Fraction at the Minimum Bubbling Point and the Set of Independent-Variable Dimensionless Groups

Variable entered	Standard error	Multiple correlation coefficient	't' values on the parameter estimates: ψ	$\frac{\rho_f\gamma D_p^3}{\mu^2}$	$\frac{\rho_p}{\rho_f}$
γ	0.017	0.863	9.9		
ψ, $\rho_f\gamma D_p^3/\mu^2$	0.015	0.904	10.6	3.6	
ψ, $\rho_f\gamma D_p^3/\mu^2$, ρ_p/ρ_f	0.009	0.968	15.5	9.7	7.7

Table 4. A Comparison Between the Data of Leva (1959) and Becker (1961) and the Predictions of Equation (8) for the Void Fraction at the Points of Minimum Fluidization and Minimum Bubbling. Fluidization with Air

Author	Material	D_p, mm	ρ_p, kg/m³	ψ	ϵ_{mf}, measured	ϵ_{mb}, predicted
Leva	Sharp sand	0.05	2700	0.67	0.60	0.62
		0.07			0.59	0.60
		0.10			0.58	0.58
		0.20			0.54	0.55
		0.30			0.50	0.53
		0.40			0.49	0.52
	Round sand	0.05		0.86	0.56	0.52
		0.07			0.52	0.51
		0.10			0.48	0.48
		0.20			0.44	0.46
		0.30			0.42	0.44
	Coal	0.05	1600	0.63	0.62	0.66
		0.07			0.61	0.64
		0.10			0.60	0.63
		0.20			0.56	0.59
		0.30			0.53	0.57
		0.40			0.51	0.55
Becker	Corn	6.92	1260	0.75	0.412	0.385
	Peas	6.65	1380	1.00	0.395	0.313
	Wheat	3.38	1380	0.91	0.380	0.355
	Rapeseed	1.61	1120	1.00	0.371	0.358
	Ottawa sand	0.76	2660	0.98	0.381	0.371

TABLE 5. COMPARISON OF MEASURED AND PREDICTED VALUES OF THE MINIMUM FLUIDIZATION VELOCITY AND THE MINIMUM BUBBLING VELOCITY. FLUIDIZATION OF GLASS BEADS WITH AIR, $Re < 10$

	Present results		Leva	Davidson	Rowe	Present results			Ergun
	Measured	Eq. (16)	Eq. (18)	Eq. (19)	Eq. (20)	Measured		Eq. (7)	Eq. (10)
D_p, mm	v_{mf}, cm/s	v_{mf}, cm/s	v_{mf}, cm/s	v_{mf}, cm/s	v_{mf}, cm/s	ϵ_{mb}	v_{mb}, cm/s	v_{mb}, cm/s	v_{mb}, cm/s
0.100	1.26	1.16	1.09	1.50	1.06	0.422	1.21	1.21	1.14
0.165	2.81	2.86	2.76	4.12	2.93	0.410	2.75	2.90	2.81
0.297	7.86	8.09	8.01	13.3	9.45	0.399	7.41	8.01	8.24
0.481	17.9	19.1	19.4	35.2	24.9	0.393	17.4	18.5	20.6

$$\left(\frac{\psi D_p(-\Delta P/H)}{\rho_f v^2}\right)\left(\frac{\epsilon^3}{1-\epsilon}\right) = 150\,\frac{1-\epsilon}{\psi Re} + 1.75 \qquad (9)$$

In fluidization, $-\Delta P/H \simeq \gamma(1-\epsilon)$. At the minimum bubbling point, $v = v_{mb}$ and $\epsilon = \epsilon_{mb}$. Thus (9) gives

$$v_{mb} = \frac{\psi^2 \epsilon_{mb}^3}{150(1-\epsilon_{mb})}\left(\frac{\gamma D_p}{\rho_p}\right)^{0.5}\left(\frac{\rho_p \gamma D_p^3}{\mu^2}\right)^{0.5} \qquad (10)$$

for creeping flow, $Re_{mb} < 10$, and

$$\gamma D_p/\rho_f v_{mb}^2 = 1.75/\psi\epsilon_{mb}^3 \qquad (11)$$

for fully developed turbulent flow.

Table 5 shows a comparison between (10) and the present results for the case of glass beads fluidized with air. The values of v_{mb} calculated from (10) with the experimental values of ϵ_{mb} are in good agreement with the experimental values of v_{mb}. This indicates that the configurational effects on particles in the bed associated with expansion to the point of minimum bubbling do not greatly affect the constants in the Ergun equation. Hence the equation can be used to predict v_{mb}, provided that realistic values of ϵ_{mb} are employed.

For $\epsilon_{mb} = 0.39$, a typical value for large, nearly-round particles, Table 4, and $\psi = 0.9$, an average value for the present materials, the right-hand side of (11) gives $1.75/\psi\epsilon_{mb}^3 = 29.5/\psi = 32.8$. This agrees well with the constant 35.4 in (5). Figure 4 shows, however, that the present results did not extend far into the turbulent flow region, and the constant 35.4 is based on extrapolation from a rather small quantity of data. Since Ergun's equation is better established than (5) for high *Re*, a value of $29.5/\psi$ can be adopted.

Over the range of the present data, $0.41 < \epsilon_{mb} < 0.52$,

$$\epsilon_{mb}^3/(1-\epsilon_{mb}) \simeq 3.5\,\epsilon_{mb}^{3.82} \qquad (12)$$

to a good approximation. With this substitution for $\epsilon_{mb}^3/(1-\epsilon_{mb})$ and with (8) for ϵ_{mb}, the Ergun result for creeping flow (10) gives

$$v_{mb} = 0.00303\,\psi^{-0.75}\left(\frac{\gamma D_p}{\rho_p}\right)^{0.5}\left(\frac{\rho_p\gamma D_p^3}{\mu^2}\right)^{0.399}\left(\frac{\rho_p}{\rho_f}\right)^{0.031} \qquad (13)$$

which can be compared with (6).

A final method of comparison is to accept (7) for v_{mb} in creeping flow. Equations (7), (10), and (12) yield

$$\epsilon_{mb} = 0.570\,\psi^{-0.52}\,(\mu^2/\rho_p\gamma D_p^3)^{0.0236} \qquad (14)$$

The differences between this formula and (8) appear to be insignificant in relation to the present data.

MINIMUM FLUIDIZATION POINT

Method

The 10-cm diam. column was used for all runs. A fixed weight of material, 1.35 kg, was put in the column. This gave a ratio of settled bed height to column diameter H_s/D of about 1.0 for sand and glass beads. The bed was fully fluidized; the gas flow was then slowly reduced in small decrements, and the pressure drop across the bed was determined as a function of the flow rate.

The pressure drop was plotted against the superficial velocity on log-log graph paper, and the point of intersection of the pressure-drop line for fully established fluidization with the line for the fixed bed condition was taken as the minimum fluidization point. This definition is illustrated in Kunii and Levenspiel's book (1969, p. 74).

Correlations for v_{mf}

The scheme followed to develop dimensionless correlations for the minimum fluidization velocity was the same as that for the minimum bubbling velocity. The results are shown in Figures 5 and 6. A correlating equation of the same general form as (4) was fitted by a nonlinear least-squares procedure, giving

$$\frac{\gamma D_p}{\rho_f v_{mf}^2} = 2.42 \times 10^5\left(\frac{\mu^2}{\rho_f\gamma D_p^3}\right)^{0.85}\left(\frac{\rho_p}{\rho_f}\right)^{0.13} + 37.7 \qquad (15)$$

$0.01 < Re_{mf} < 1000$, $500 < \rho_p/\rho_f < 50000$, and $1 < \rho_f\gamma D_p^3/\mu^2 < 10^7$. The residual variance indicates that v_{mf} is predicted within ± 37% (95% confidence interval) over the range of the data.

For creeping flow, (15) reduces to

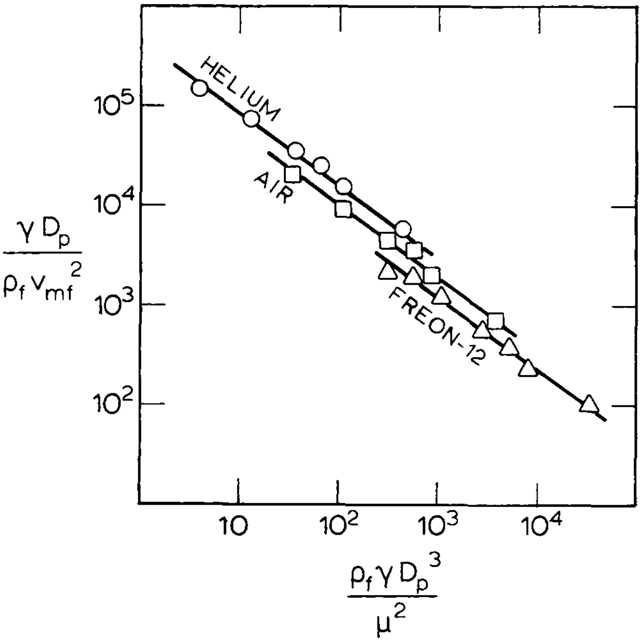

Fig. 5. The relation between the dimensionless minimum fluidization velocity and $\rho_f\gamma D_p^3/\mu^2$. Systems are sand, $\psi = 0.85$, $D = 10$ cm, $H_s/D = 1$, fluidization with helium, air, and freon-12.

$$v_{mf} = 0.00203 \left(\frac{\gamma D_p}{\rho_p}\right)^{0.5} \left(\frac{\rho_p \gamma D_p^3}{\mu^2}\right)^{0.425} \left(\frac{\rho_p}{\rho_f}\right)^{0.01} \tag{16}$$

For air/sand systems at 20°C and 1 atm, $\rho_p/\rho_f = 2200$, and (16) gives

$$v_{mf} = 0.00219 \left(\frac{\gamma D_p}{\rho_p}\right)^{0.5} \left(\frac{\rho_p \gamma D_p^3}{\mu^2}\right)^{0.425} \tag{17}$$

The effect of ρ_p/ρ_f in (16) is insignificant, and the differences between the predictions of (16) and (17) are negligible.

Comparison with v_{mb}

The minimum fluidization velocity is about the same as, or slightly greater than, the minimum bubbling velocity. The data in Table 5 are fairly typical. The behavior of v_{mf} is, however, more erratic, and this is reflected in the greater deviations of the data on v_{mf} from (15) compared to those on v_{mb} from (5)—v_{mf} is predicted within ± 37% with 95% confidence, whereas v_{mb} is predicted within ± 25%. It appears that the minimum bubbling point is definitely better defined than the minimum fluidization point. The problem with the latter is that the fraction void and particle configuration in the fixed bed which is formed when the gas flow is gradually reduced below the fluidization level are sensitive to the rate of reduction of the flow and to any jarring or vibration of the bed. This affects the relation between pressure drop and flow rate, and hence the value obtained for v_{mf}.

For practical purposes, v_{mb} is the critical velocity for aggregative fluidization, and v_{mf} is simply a characteristic that happens to approximate v_{mb}. When the bed behavior tends toward particulate fluidization, however, then v_{mf} is the most reasonable measure of the superficial velocity for the onset of fluidization.

Comparison with Other Work

The equations of Leva (1959), Davidson (1963), and Rowe (1961) for v_{mf} in the creeping flow regime are

$$v_{mf} = 0.0007\, Re_{mf}^{-0.063}\, D_p^2 \gamma/\mu \tag{18}$$

$$v_{mf} = 0.00114\, D_p^2 \gamma/\mu \tag{19}$$

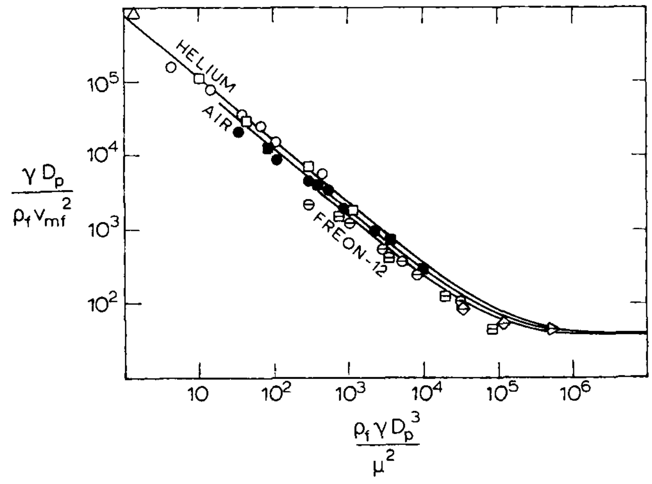

Fig. 6. The relation between the dimensionless minimum fluidization velocity and $\rho_f \gamma D_p^3/\mu^2$. Systems with D = 10 cm, 1.35 kg material in column (H_s/D = 1 for sand), fluidization with helium, air and freon-12. Materials: ○●○, sand, ψ = 0.85; □■⊟, glass beads, ψ = 1.00; ⦵, iron shot, ψ = 0.95; △, cracking catalyst, ψ = 0.95; ▷, clover seed, ψ = 0.95. Curves are given by Equation (15).

$$v_{mf} = 0.00081\, D_p^2 \gamma/\mu \tag{20}$$

$Re_{mf} < 10$. For comparison with (16), these are transformed to

$$v_{mf} = 0.00108 \left(\frac{\gamma D_p}{\rho_p}\right)^{0.5} \left(\frac{\rho_p \gamma D_p^3}{\mu^2}\right)^{0.441} \left(\frac{\rho_p}{\rho_f}\right)^{0.059} \tag{21}$$

$$v_{mf} = 0.00114 \left(\frac{\gamma D_p}{\rho_p}\right)^{0.5} \left(\frac{\rho_p \gamma D_p^3}{\mu^2}\right)^{0.5} \tag{22}$$

$$v_{mf} = 0.00081 \left(\frac{\gamma D_p}{\rho_p}\right)^{0.5} \left(\frac{\rho_p \gamma D_p^3}{\mu^2}\right)^{0.5} \tag{23}$$

Leva's equation, like (16), represents a correlation of experimental data, whereas Davidson's and Rowe's are based on theoretical arguments in which the fraction void of the bed is assumed to be a constant at the point of minimum fluidization.

The agreement between Leva's result, (21), and ours, (16), as to the exponent on $\rho_p \gamma D_p^3/\mu^2$ is reasonably good. These empirical observations indicate that the value of the exponent given by simple theory, 1/2, is significantly in error.

The absolute differences between the predictions of (16), (21), (22), and (23) are best illustrated by an example, Table 5. It is seen that for uniform-sized spherical glass beads fluidized with air, Davidson's equation significantly overpredicts the measured values of v_{mf}. Rowe's equation gives better results but tends to underpredict for small particles and overpredict for large ones. Leva's equation is in reasonably good agreement with all the data in the example, and the difference in accuracy between it and the present equation appears to be small—perhaps insignificant.

MINIMUM SLUGGING POINT

The onset of slugging represents the terminal stage of bubble coalescence, when a bubble spans the entire cross section of the column. Past studies relating to the minimum slugging point have been inconclusive, and no comprehensive study has hitherto been reported. The most frequently used criterion is that proposed by Stewart and Davidson (1967),

$$v_{ms} - v_{mf} \leq 0.2(0.35\sqrt{gD}) \tag{24}$$

A significant limitation of this relation is that, from the nature of the underlying assumptions, reasonable results can be expected only if H_s/D is greater than 3 or 4. The assumptions, concerning the slug spacing and the slug volume, are themselves open to question, particularly for large beds. However, because (24) agrees roughly with the data of several authors, it has been accepted as the best available guideline.

A problem that has caused considerable ambiguity is that no standard definition of the onset of slugging has been established. The results reported are thus affected by each author's interpretation of the phenomena.

The object of the present study was to obtain a comprehensive set of data relating to the minimum slugging point and to develop from these a correlation which contains all significant parameters of the fluid bed system, does not require knowledge of other dependent variables for its use, and is based on a clear and unique definition of the phenomenon.

Method

The following operational definition of the slugging point was adopted: the point of minimum slugging is reached when bubbles, before they arrive at the top of the bed, are seen to have a continuous floor around the circumference of the column, as shown in Figure 7. Using this definition, it was easy to observe the slugging point in beds with $H_s/D > 2$, and measurements of the minimum slugging velocity were reproducible with good precision. At $H_s/D < 2$, the observations became increasingly difficult with decreasing H_s/D, due to the high degree of bed turbulence. Observations at $H_s/D < 1$ were impossible for most systems excepting those with very large or heavy particles, such as metal shot.

The procedure followed in establishing the minimum slugging point was to raise the gas flow rate to a point where slugging was readily apparent. The flow was then gradually decreased until the formation of bubbles of the shape shown in Figure 7 approached the vanishing point. Strong illumination of the column was required to ensure that bubbles of the required characteristics, that is, incipient slugs, were easily recognized. Observations were generally repeated ten times when fluidizing with air, and five times with helium and freon-12. The minimum slugging velocity was measured in all four columns in beds of the various sand particles with H_s/D ranging from 1 to 60.

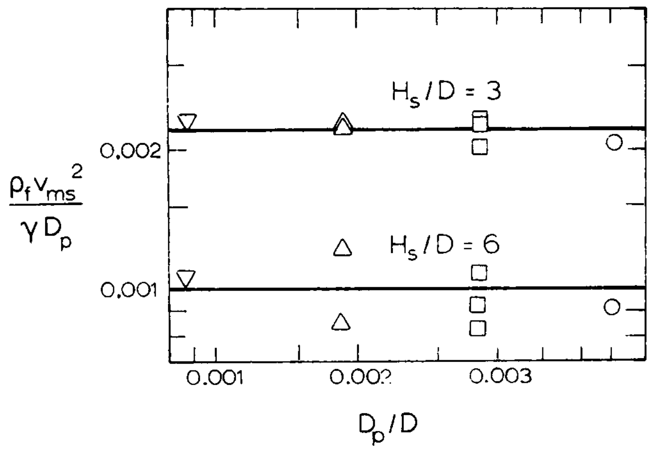

Fig. 8. The effect of D_p/D on the dimensionless minimum slugging velocity. Systems are sand/air, $\psi = 0.85$, $D_p = 0.18$ mm, and $H_s/D = \{3, 6\}$. Column diameters D, cm: ○, 2.5; □, 5; △, 10; ▽, 21.

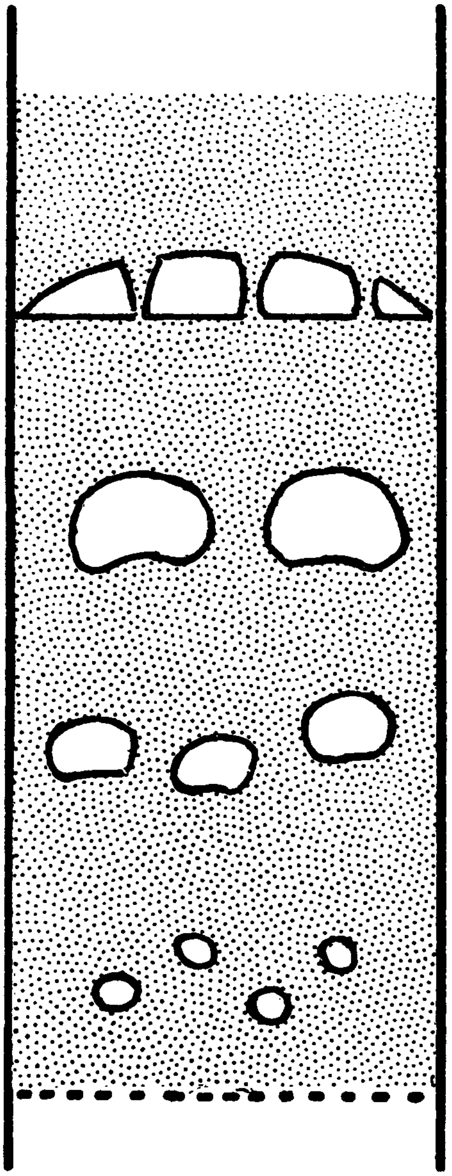

Fig. 7. A fluid bed at the onset of slugging. The uppermost bubble formation has a continuous floor and is taken to be an incipient slug. The fingers of dense phase reaching down to the floor of the slug are streams of particles flowing back along the column wall. There is also a rain of particles from the roof of the slug to the floor.

Characteristics of fluidization at the onset of slugging can also be established by instrumental, rather than visual, means by spectral analysis of pressure fluctuations at the foot of the bed. Extensive studies of pressure fluctuations were carried out in another phase of the present research (Broadhurst, 1972); these results will appear in another paper.

Effect of D_p/D

The effect of D_p/D was investigated with one sand, $D_p = 0.18$ mm, with air as the fluidizing medium, at H_s/D values of 3 and 6, in all four columns. In effect, $\rho_f\gamma D_p^3/\mu^2$, ρ_p/ρ_f, ψ, and H_s/D were held constant while D_p/D was varied. The results, Figure 8, indicate that $\rho_f v_{ms}^2/\gamma D_p$ is constant over the experimental range of D_p/D. Regression analysis confirmed the insignificance of D_p/D. This conclusion, which suggests that the minimum slugging point need be studied at only one column diameter, saved much labor. However, as a precautionary measure, the 5-cm and 10-cm inside diameter columns were both used in all subsequent experimental work.

Effect of ψ

The effect of particle shape was studied with spherical glass beads, $D_p = 0.16$ mm and $\psi = 1$, and with sand, $D_p = 0.15$ mm and $\psi = 0.85$, in beds fluidized with air. The groups $\rho_f\gamma D_p^3/\mu^2$ and ρ_p/ρ_f were effectively the same for these systems. The results, Figure 9, indicate that ψ has little effect on the minimum slugging velocity over the range studied. Regression analysis confirms the insignificance of ψ.

Effect of $\rho_f\gamma D_p^3/\mu^2$, ρ_p/ρ_f and H_s/D

The values of $\rho_f\gamma D_p^3/\mu^2$ and H_s/D were varied through D_p and H_s, and the density ratio ρ_p/ρ_f was varied through ρ_f.

Some of the data for fluidization with air are shown in Figure 10. It appears that at small values of H_s/D, $\rho_f v_{ms}^2/\gamma D_p$ is independent of $\rho_f\gamma D_p^3/\mu^2$, and depends only on H_s/D. This conclusion is further supported by the data for fluidization with helium and freon-12. However, the group ρ_p/ρ_f has a significant effect over the whole range of H_s/D.

A second conclusion indicated by Figure 8 is that at high values of H_s/D, the group $\rho_f v_{ms}^2/\gamma D_p$ approaches a constant value which is independent of H_s/D, but dependent on $\rho_f\gamma D_p^3/\mu^2$ and ρ_p/ρ_f.

The existence of two regimes is thus indicated, one in shallow beds where $\rho_f v_{ms}^2/\gamma D_p$ depends only on H_s/D and ρ_p/ρ_f, and the other in deep beds where it depends on $\rho_f\gamma D_p^3/\mu^2$ and ρ_p/ρ_f. This suggests a model of the form

$$\frac{\rho_f v_{ms}^2}{\gamma D_p} = A1\left(\frac{H_s}{D}\right)^{A2}\left(\frac{\rho_p}{\rho_f}\right)^{A3} + A4\left(\frac{\rho_f\gamma D_p^3}{\mu^2}\right)^{A5}\left(\frac{\rho_p}{\rho_f}\right)^{A6} \quad (25)$$

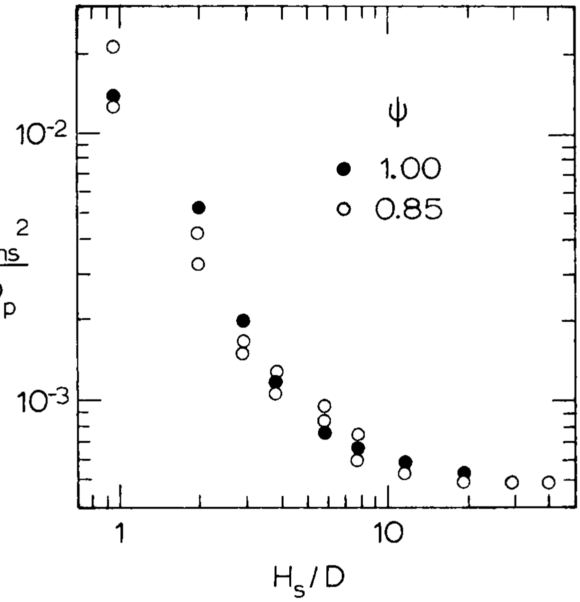

Fig. 9. The effect of particle shape on the relation between the dimensionless minimum slugging velocity and H_s/D. Systems with $D = 10$ cm, fluidization with air. Materials: ○, sand, $D_p = 0.15$ mm, $\psi = 0.85$; ●, glass beads, $D_p = 0.16$ mm $\psi = 1.00$.

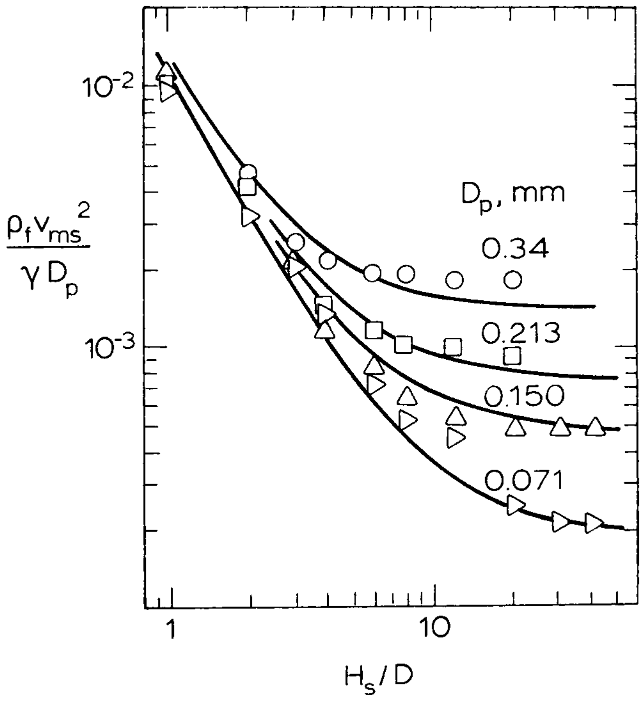

Fig. 10. The dimensionless minimum slugging velocity as a function of H_s/D and particle diameter. Systems are sand/air, $\psi = 0.85$, $D = 10$ cm. Particle diameters D_p, mm: ○, 0.343; □, 0.213; △, 0.150; ▷, 0.071. Curves are given by Equation (30).

The parameters $A1$ to $A6$ were evaluated by a nonlinear least squares procedure to minimize the sum of the squares of the residuals. The final correlation is

$$\frac{\rho_f v_{ms}^2}{\gamma D_p} = 51.4\left(\frac{D}{H_s}\right)^{1.79}\left(\frac{\rho_f}{\rho_p}\right)^{1.09} + 0.00416\left(\frac{\rho_f\gamma D_p^3}{\mu^2}\right)^{0.41}\left(\frac{\rho_f}{\rho_p}\right)^{0.59} \quad (26)$$

$1 < H/D < 40$, $500 < \rho_p/\rho_f < 15000$, and $1 < D_p^3\gamma\rho_f/\mu^2 < 40000$. The residual variance indicates that v_{ms} can be predicted within $\pm$ 25% (95% confidence interval) over the whole range of the data. A comparison between (26) and data for fluidization with air is shown in Figure 10.

For $H_s/D < 3$, (26) reduces to

$$v_{ms} = 7.17\,(D/H_s)^{0.895}\,(\gamma D_p/\rho_p)^{0.5}\,(\rho_f/\rho_p)^{0.045} \quad (27)$$

Inserting the value of ρ_p/ρ_f for air/sand at 20°C and 1 atm, 2200, this approximates to

$$v_{ms} = 5.07\,(D/H_s)^{0.895}\,(\gamma D_p/\rho_p)^{0.5} \quad (28)$$

The actual effect of ρ_p/ρ_f in this regime may be altogether insignificant.

For $H_s/D > 20$, (26) gives

$$v_{ms} = 0.065\,(\gamma D_p/\rho_p)^{0.5}\,(D_p^3\gamma\rho_p/\mu^2)^{0.205} \quad (29)$$

Here no effect of ρ_p/ρ_f is predicted. The above conclusions suggest that (26) should be rewritten in the form

$$\frac{\rho_p v_{ms}^2}{\gamma D_p} = 51.4\left(\frac{D}{H_s}\right)^{1.79}\left(\frac{\rho_f}{\rho_p}\right)^{0.09} + 0.00416\left(\frac{\rho_p\gamma D_p^3}{\mu^2}\right)^{0.41} \quad (30)$$

and this is a recommended form of the correlation. For the systems, here studied, $\rho_f/\rho_p << 1$, in which case $\rho_p v_{ms}^2/\gamma D_p = v_{ms}^2/gD_p$. Thus the left-hand side of (30) is, in effect, the Froude number.

Evaluation of the constants and exponents in (25) with H_s/D replaced by H_0/D gave the result, in the form analogous with (30),

$$\frac{\rho_p v_{ms}^2}{\gamma D_p} = 129\left(\frac{D}{H_0}\right)^{1.79}\left(\frac{\rho_f}{\rho_p}\right)^{0.09} + 0.00416\left(\frac{\rho_p\gamma D_p^3}{\mu^2}\right)^{0.41} \quad (31)$$

The transformation between (30) and (31) is simply $H_0 = H_s(1 - \epsilon_s)$, $\epsilon_s = 0.40$. Thus, as noted earlier, the results of analysis of the present set of data are indifferent to the distinction between H_0 and H_s. Equation (31) is a second recommended form of the correlation for the minimum slugging velocity and is preferable to (30) in the sense that H_0 is an independent variable, whereas H_s, strictly speaking, is not.

Comparison with Other Work

Rearrangement of the relation of Stewart and Davidson (1967), (24) gives

$$\rho_f v_{ms}^2/\gamma D_p = (0.07\sqrt{gD} + v_{mf})^2\,(\rho_f/\gamma D_p) \quad (32)$$

where the possible inequality in (24) is ignored for the moment. A comparison between some of the present data and (32) is shown in Figure 11. According to (32), $\rho_f v_{ms}^2/\gamma D_p$ should change with D but not H_s, whereas the present results indicate that it varies with H_s/D or not at all, as shown by (26).

In deriving their criterion, Stewart and Davidson stressed its tentative nature and indicated the need for further verification of the assumed slug flow pattern. Their basic assumption was that slugs are of height D and are spaced at intervals of length 3 D. This spacing was suggested by experiments with a small column, 0.63-cm diameter by 6 cm high, and very roughly agrees with slug frequencies observed in the present work (Broadhurst, 1962). However, the assumption that slugs at the onset of slugging are of height D is either weak or quite wrong, based on the present observations. The slug height in our 10-cm column was always considerably less than D. This was true also for all columns with beds of particles with $D_p <$ 0.15 mm. Only in deep beds of coarse particles did the slug height approximate D.

It may be noted that in the form they proposed it, (24), Stewart and Davidson's relation is empirically correct; over the range of the present data, it never predicts minimum slugging velocities lower than the observed values. Unfortunately, the trend of the predictions is in the wrong direction; a conservative relation of the form of (24) would, since slugging is normally an undesirable condition, always predict values of v_{ms} smaller than, or equal to, the observed values.

The general form of the present results, and particularly the effect of H_s/D, is supported by the work of Kehoe (1969, 1970) and Kehoe and Davidson (1972). Kehoe reports that the height of a slug is typically 0.6 D, and may be less. The stable slug spacing is typically 3 D in beds of coarse particles, in agreement with Stewart and Davidson's assumption, but can be much larger in beds of fine particles. Stable slug spacing occurs, moreover, only when H_s/D is adequately large, and the required value of H_s/D is greater for fine particles. In the regime at smaller values of H_s/D, the slug spacing is less than the stable one. Kehoe (1969) presents appropriate modifications of the model of Stewart and Davidson for these regimes. His qualitative observations are in reasonable agreement with the present results.

ACKNOWLEDGMENTS

The work was supported by grants from the National Research Council of Canada. T. E. Broadhurst received personal support from the Royal Military College of Canada, Kingston, Ontario. The material on minimum bubbling and slugging was presented at the Congrès International "La Fluidisation et ses Application", Toulouse, France, 1973 (Broadhurst and Becker, 1973) and we are grateful to the Société de Chimie Industrielle for permission to publish in the *AIChE Journal*.

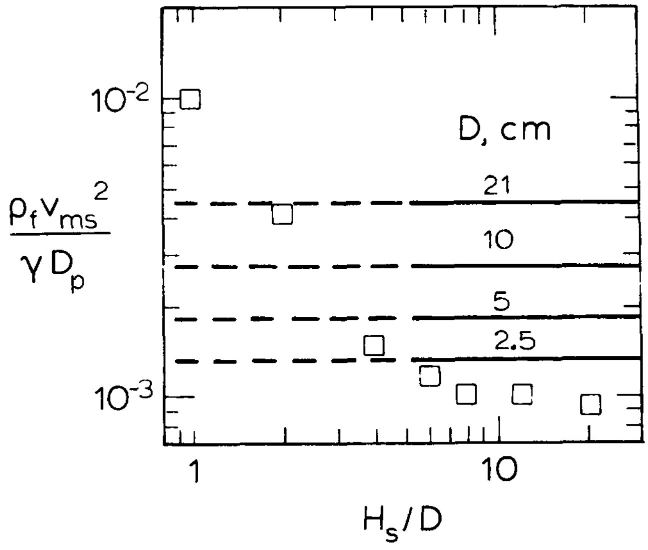

Fig. 11. A comparison between the limit predictions of Stewart and Davidson's equation, (26), for the minimum slugging velocity (horizontal lines), and the present data. The systems are sand/air, D_p = 0.213 mm, D = {5 cm, 10 cm}. Each point, □, represents the result for both column diameters D at constant H_s/D, the effect of D being insignificant. The dashed portions of the Stewart and Davidson prediction indicate the region, approximately $H_s/D > 5$, in which their assumptions cannot be expected to hold.

NOTATION

D = column diameter
D_p = particle diameter
g = acceleration due to gravity
H = bed height
H_0 $\equiv H(1 - \epsilon)$, height equivalent to the solid matter in the bed
P_1 = pressure in the gas above the bed
v = superficial fluid velocity
γ $\equiv g(\rho_p - \rho_f)$, specific weight of particles minus their specific buoyancy
ψ $\equiv (6V_p/\pi)^{2/3}/(S_p/\pi)$, particle sphericity ($V_p$ = volume, S_p = surface area)
ϵ = void fraction
ρ = density
μ = viscosity of fluid

Subscripts

f = a fluid property
mb = a property measured at the minimum bubbling point
mf = a property measured at the minimum fluidization point
ms = a property measured at the minimum slugging point
p = a particle property
s = a property of a "settled bed," the fixed bed obtained by vibrating a bed until no further consolidation takes place

LITERATURE CITED

Becker, H. A., "An Investigation of Laws Governing the Spouting of Coarse Particles," *Chem. Eng. Sci.*, **13**, 245 (1961).
Broadhurst, T. E., "Particle Motion, Slugging, and Pressure Fluctuation Phenomena in Fluidized Beds," Ph.D. thesis, Queen's University, Kingston, Ontario (1972).
———., and H. A. Becker, "The Application of the Theory of Dimensions to Fluidized Beds," Proc. of Toulouse, France, Intern. Cong. on Fluidization and Its Applications, pp. 10-27, Société de Chimie Ind. (1973).
Davidson, J. F., and D. Harrison, *Fluidized Particles*, Cambridge University Press, England (1963).
Ergun, S., "Fluid Flow Through Packed Columns," *Chem. Eng. Prog.*, **48**, 89 (1952).
Kehoe, P. W. K., "The Effect of Particle Size on Slugging Fluidized Beds," Ph.D. thesis, University of Cambridge, England (1969).
———., "A Strategy for the Design of Fluidized Bed Chemical Reactors," *Chem. Enginer, Nos. 235-244*, CE437 (1970).
———., and J. F. Davidson, "The Fluctuation of Surface Height in Freely Slugged Fluidized Beds," 74th Ann. Meeting of the AIChE, St. Louis, Missouri (1972).
Leva, M., *Fluidization*, McGraw-Hill, New York (1959).
Kunii, D., and O. Levenspiel, *Fluidization Engineering*, Wiley, New York (1969).
Romero, J. B., and L. N. Johansen, "Factors Affecting Fluidized Bed Quality," *Chem. Eng. Progr. Symp. Ser.*, **58**, 28 (1962).
Rowe, P. N., "Drag Forces in a Hydraulic Model of a Fluidized Bed—Part II," *Trans. Instn. Chem. Engrs.*, **39**, 175 (1961).
Stewart, P. S. B., and J. F. Davidson, "Slug Flow in Fluidized Beds," *Powder Technol.*, **1**, 61 (1967).
Wilhelm, R. H., and M. Kwauk, "Fluidization of Solid Particles," *Chem. Eng. Progr.*, **44**, 201 (1948).

Manuscript received June 4, 1974; revision received and accepted November 13, 1974.